

BSc Thesis Biomedical technology

Channel reduction for EEG recordings of nociceptive evoked brain activity

R. J. Poelarends

Supervisors:

B. van den Berg

J. R. Buitenweg

Committee:

B. van den Berg

J. R. Buitenweg

J. Rouwkema

June, 2022

Department of Biomedical Signals and Systems

Faculty of Electrical Engineering, Mathematics and Computer Science

Biomedical Engineering

1 Abstract

EEG is a useful method to assess sensory deficits in chronic pain patients. One of the barriers for widescale use of EEG in a clinical context is the required time and training for applying a 32+ channel EEG cap. In this work, it is investigated whether the number of EEG channels can be reduced to four without losing important nociceptive evoked brain activity. Artifact removal from EEG recordings is a major challenge in a few-channel scenario, since most existing techniques cannot guarantee efficient and effective artifact removal performance. Consequently, I propose Noise-Assisted Fast Multivariate Empirical Mode Decomposition combined with Canonical Correlation Analysis (NA-FMEMD-CCA) to remove EMG and EOG artifacts from the preselected T7, Cz, T8 and Fz EEG channels. The performance of the proposed method is compared with the currently used artifact removal method, Independent Component Analysis (ICA), and evaluated using power spectral density, visual signal-inspection and deep learning. The results demonstrate that the four preselected channels contain the important nociceptive evoked brain activity. The proposed method removes all eye-movement artifacts, but is yet unable to remove very intense spiking eye-blink artifacts and EMG artifacts properly. In addition, NA-FMEMD-CCA currently removes parts of important nociceptive evoked brain activity content. Parameter tuning is required to optimise the artifact removal method performance and preserve all nociceptive evoked brain activity content. Therefore, it can be concluded that four channel EEG can be used in order to make EEG more applicable for widescale use in the clinic, yet the artifact removal method requires further investigation to be applicable.

2 Introduction

Chronic pain affects the life of 19% [1] of adult Europeans, which makes it a leading source of human suffering and disability [2]. Pain can be classified as nociceptive, inflammatory or neuropathic (NP) [3] and is called chronic when it persists or recurs for longer than three months [4]. Under normal circumstances, the perception of pain, a biopsychosocial phenomenon, occurs when a nociceptor (pain receptor) is activated by a thermal, mechanical or chemical stimulus. Chronic pain patients can also perceive pain without activation of nociceptors. The intensity of stimulation at which pain is perceived depends on the nociceptive threshold. Depending on the type and intensity of the stimulus, A δ fibers or C fibers will be activated, resulting in a sharp pricking and intense burning subjective experience of pain, respectively [5][6].

Subjectiveness of pain complicates identification of impaired nociceptive processing and therefore complicates treatment of chronic pain patients [7]. Van den Berg *et al.* [8] recently developed a method to assess nociceptive processing and evaluate nociceptive detection thresholds, which allowed them to record nociceptive detection thresholds and evoked potentials (EP) using intra-epidermal electric stimulation, in which the participants had to indicate whether a stimulus was experienced. In 2022, Van den Berg *et al.* [9] proposed a new non-invasive method in which perceptual thresholds were estimated based on EEG alone using a deep neural network, instead of using the participants indication. In the future, this EEG-based development can support diagnosis and treatment of chronic pain patients.

Problem statement

A barrier for such widescale use of EEG to assess sensory deficits in a clinical context is the required time (20 - 40 minutes) and significant training for applying an 32+ channel EEG cap. Reduction of the number of channels is required to be able to use electroencephalography (EEG) to support diagnosis in a clinical setting. The use of a 32+ channel EEG cap brings benefits in removing EMG, ECG and ocular artifacts and effectively capturing the full signal of all active brain areas. As such, one of the main challenges of using EEG to support diagnosis in a clinical setting, is to reduce the number of required channels, while preserving the ability to clean the signals and preserving as much information as possible about activated brain areas.

Research goal

The main goal in this thesis is to study whether we can acquire clean EEG responses to nociceptive stimuli using only the T7, Cz, T8 and Fz EEG channels. The strategy is to first select and implement an approach to remove EMG and ocular artifacts using the four preselected channels. The selected methods will be evaluated using an existing set of 32-channel EEG recordings, where in addition new EEG recordings from four participants will be acquired for additional testing. The cleaned signals using the limited set of channels will be compared to the cleaned signals using the full 32 channels, to evaluate if the signals are altered. Finally, a deep neural network

will be used to assess whether information in the signal about stimulus perception is reduced.

Thesis outline

The first section of this thesis is the background section, which provides necessary information about the context of the research and elaborates upon the concepts and techniques mentioned in this thesis. The method section discusses the used approach to removing artifacts in a few-channel scenario and the comparison between the currently used method and the proposed approach. In the results section, both methods will be compared in terms of capability of artifact removal and nociceptive evoked brain activity preservation, to evaluate if the artifact removal method is serviceable in few-channel EEG. In the discussion section, I will evaluate the performance of the proposed method to determine if the previously mentioned goal was reached. Furthermore, conclusions will be drawn in the conclusion section.

3 Background

This section gives an overview of the characteristics of EEG of nociceptive evoked brain activity and types of artifacts that may affect the EEG-recordings. Also, possible artifact removal techniques under few-channel scenarios and evaluation methods of proposed approach are discussed.

Characteristics of EEG of nociceptive evoked brain activity

EEG is a method to measure voltage as a result of neuronal interactions. Using electrodes attached to the scalp, the electrical activity of the surface layer of the brain is being measured. The measured signal consists of multiple periodic signals at frequencies from 0.01 Hz to around 100 Hz [10] and can be divided into multiple rhythms of different frequencies, which are summarized in Table 1. Artifacts in EEG can imitate neural information which can bias the interpretation and diagnosis in clinical research, which requires separating them from the desired signal [10][11].

EEG recordings of response to stimuli, so-called evoked potentials (EP) or event-related potentials (ERP) recordings, can be used to investigate somatosensory processing [12]. Analysis of nociceptive phase-locked EPs and non-phase-locked event-related synchronization or desynchronization (ERS or ERD) can give insight in central nervous system processing and functionality of nociceptive pathways [13]. EP components, described by the positive (P) or negative (N) polarity of the maximum amplitude and the order in which they occur in the EP, are generally characterized by latency and amplitude. For example, N1 is the first negative component and P1 the first positive component in the EP, which can be seen in Figure 1. The N1, N2 and P2 waves are thought to relate to nociceptive input processing, which makes them important components of nociceptive EPs. The optimal electrode location for recording each wave depends on the type of the wave. For example, the N1 wave is mainly measured at the temporal electrodes (T3-T6), but N2 and P2 are always measured at the central electrodes (e.g. Cz). Insight in characteristics of EPs can support diagnosis of neurological disorders. For instance, EEG signals of chronic neuropathic pain patients show decreased amplitude of the N2-P2 complex, along with increased latencies of the N2 and P2 components on nociceptive stimuli [12][14].

Table 1: Different EEG rhythms, their activity of occurring and frequency bands [11][15].

Rhythm	Activity	Frequency (Hz)
Infra slow oscillations (ISO)	Mediator of brain sub-states [16]	<0.5
Delta	Deep sleep	0.5 - 4
Theta	N1 and N2 sleep, drowsiness	4 - 7
Alpha	Awake	8 - 12
Sigma	N2 sleep	12 - 16
Beta	Active thinking	13 - 30
High-frequency oscillations (HFOs)	Possible relation with epilepsy and disorders of cortical integrity	>30

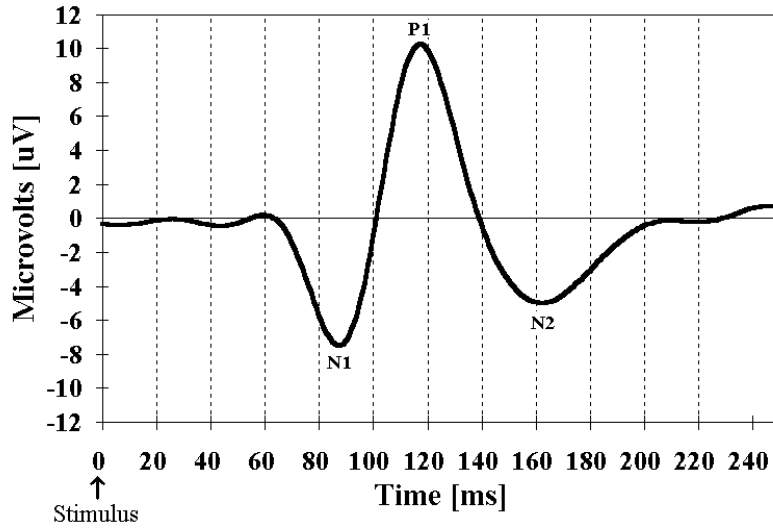


Figure 1: Evoked potential in which the characteristic N1, P1 and N2 waves are labeled [17].

Types of artifacts

The EEG signals are a mixture of cerebral activity and noise [18]. Electrical signals originating from the brain and artifacts assemble, because of capacitive coupling or the volume conduction effect, and propagate to the scalp. Artifacts are unwanted signals originated from internal and external sources. Different types of artifacts may appear as regular or irregular, in which some appear in multiple neighboring channels and others can only be found in single-channel [11]. Physiological signals from the body itself, the internal sources (e.g. eye blink, bioelectric potentials from heart beat and muscle activity, sweat), can be categorized as intrinsic artifacts [10][19]. Physiological, intrinsic artifacts may interfere with neural information, which necessitates the use of particular algorithms to remove them [10]. Extrinsic artifacts come from environmental artifacts (e.g. high electrode impedance, line noise, power supply, electrode pop-up [20]) and experiment error. Major artifacts are shown in Figure 2 and will be discussed in the following section.

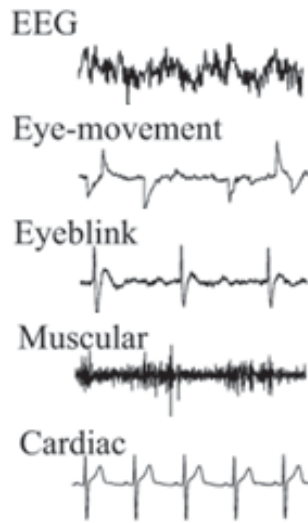


Figure 2: Major EEG artifacts [21].

Muscle artifacts

Electromyography (EMG) measures electrical activity of muscle contraction. EEG is often contaminated with EMG artifacts, due to swallowing, frowning, chewing or other muscular activities [22]. EMG distributes a spectrum between 0 Hz and 200 Hz, which makes it overlap with all classic EEG frequency bands. However, muscle artifacts are mainly present in beta rhythm [23]. Additionally, EMG can be detected in all EEG channels and is produced by functionally independent muscle groups [24][18]. Due to these characteristics it is difficult to remove muscle artifacts [24].

Ocular artifacts

The electrical activity produced by eye movement and blinking may contaminate the recorded EEG. Eye movement and blinking can be recorded using electrooculogram (EOG). The amplitude of blinking is many times greater than EEG, which makes EOG a significant artifact [25][26]. Moreover, the frequency of EOG is similar to the frequency of EEG signals, which makes it more difficult to separate [25]. However, eye-blink artifacts are mainly present in delta rhythm [23]. The amplitude of the EOG depends on the eye movement direction and electrode position. Blinking usually contaminates the EEG signal with a more abrupt change than eye movement, which causes higher frequency interference [26]. Having a reference EOG, recorded along with the EEG signal, is found very advantageous for EOG artifact removal [18]. Recording of vertical, horizontal and radial EOG is recommended, since they all propagate differently through the scalp [26].

Cardiac artifacts

Cardiac artifacts can be categorized in pulse artifacts and electrocardiogram (ECG) artifacts. Pulse artifacts may be introduced in the EEG signals when an electrode is placed near a blood vessel [10][18]. Pulse artifacts are hard to correct since the time and frequency content is similar to parts of the EEG signals [18]. The electrical activity introduced by blood flow generates slow periodic waves, with a frequency range around 1.2 Hz. Pulse artifact amplitude depend on the electrode-position [18] and thus can be minimized by proper electrode positioning [10]. ECG artifacts, as a result of cardiac activity, appear in a regular low amplitude pattern [10] in the scalp [18]. Reference channels are found to be useful for removing both pulse artifacts and ECG artifacts [10][18].

Extrinsic artifacts

Extrinsic artifacts are introduced by e.g. high electrode impedance, line noise, power supply or electrode pop-up [20]. Line noise and low frequency trends in the EEG can be easily removed using different filters due to the narrow frequency bands not interfering with the frequency band of the desired signal [18]. Experiment error can be reduced by proper procedure [10].

Artifact removal techniques under few-channel scenarios

Single artifact removal techniques, such as regression methods, blind source separation (BSS), filtering methods and decomposition technologies, are mainly insufficient for artifact removal under few-channel scenarios [10][11]. Artifact removal using BSS methods (e.g. independent component analysis (ICA) or canonical correlation analysis (CCA)) requires the number of underlying sources being smaller than the number of EEG channels [10][11][23]. BSS methods can be combined with decomposition technologies, such as wavelet transform (WT), empirical mode decomposition (EMD), ensemble EMD (EEMD), multivariate EMD (MEMD), sparse component analysis (SCA) and variational mode decomposition (VMD), to increase the number of channels and used as hybrid methods in few-channel scenarios [23]. High-density multichannel techniques require more channels than sources and single-channel techniques degrade performance as they do not make use of invaluable cross-channel interdependence, which make these kind of techniques mainly insufficient for a four channel scenario [27].

Possible suitable artifact removal techniques for few-channel scenarios are shown in Table 2. According to literature, MEMD-CCA, NA-FMEMD-CCA and MEMD-IVA are all able to remove EMG artifacts, but the ability to remove eye-blink artifacts and white noise is only proven for NA-FMEMD-CCA. The signal length ranges in Table 2 are the useful signal lengths for every method, using a sample frequency between 256 and 512 Hz. The computational time labels are based on the relative computational time of MEMD and FMEMD. Computational time of both methods that use MEMD are labeled as 'high', since MEMD-CCA takes on average 23.91 seconds to remove artifacts from a 2560 sample EEG signal, while FMEMD-CCA takes on av-

erage only 1.55 seconds to compute. CCA takes on average 0.04 seconds, from which it can be concluded that the computational time difference between MEMD and FMEMD is significant, while the contribution of CCA or IVA to the total computational time is small [28]. The number of channels represent the number of EEG channels that are proven useful for each method.

Table 2: Characteristics of Multivariate EMD-CCA (MEMD-CCA), Noise-assisted fast multivariate EMD-CCA (NA-FMEMD-CCA) and Multivariate EMD independent vector analysis (MEMD-IVA) as few-channel EEG artifact removal methods.

Method	Type of artifacts	Signal length (samples)	Computational time	Number of channels
MEMD-CCA [27][28]	EMG	2048 - 10240	High	1-8
NA-FMEMD-CCA [23][28]	EMG, Eye-blink, white noise	2048 - 2560	Low	1-8
MEMD-IVA [29]	EMG	2500 - 5000	High	1-8

The aim of this thesis is to study whether we can acquire clean EEG responses to nociceptive stimuli using only four pre-selected EEG channels. This requires an effective and efficient artifact removal technique, since the signal needs to be cleaned quick and properly to be able to use it in a clinical setting. One artifact removal method is chosen from in Table 2, based on effectiveness and efficiency. NA-FMEMD-CCA seems the most promising artifact removal technique in a few-channel scenario, since NA-FMEMD-CCA has the lowest computational time and has the ability to remove most types of artifacts. The chosen artifact removal method, NA-FMEMD-CCA, will be further elaborated below and evaluated in this thesis as an artifact removal method in a few-channel scenario.

Overview of NA-FMEMD-CCA artifact removal approach

NA-FMEMD-CCA is a suitable hybrid method for artifact removal in cases where the number of channels is too small for blind source separation methods. NA-FMEMD-CCA denoises channels while taking cross-channel interdependence information into account. Power Spectral Density (PSD) plots show that this method is able to largely suppress EMG and almost completely remove eye-blink artifacts while preserving the ground truth EEG. One of the advantages of NA-FMEMD-CCA is the small computational time, which is five times smaller compared to other MEMD methods, which makes it suitable for real-time processing [23].

The approach of artifact removal using NA-FMEMD-CCA, which is illustrated in Figure 3, consists of four main steps:

1. Decompose the EEG signals into multivariate IMFs by applying NA-FMEMD.
2. Unmix the EEG signals into their original sources using CCA.
3. Select and reject artifact sources based on autocorrelations.
4. Reconstruct the artifact-free EEG using inverse CCA and uncontaminated IMFs.

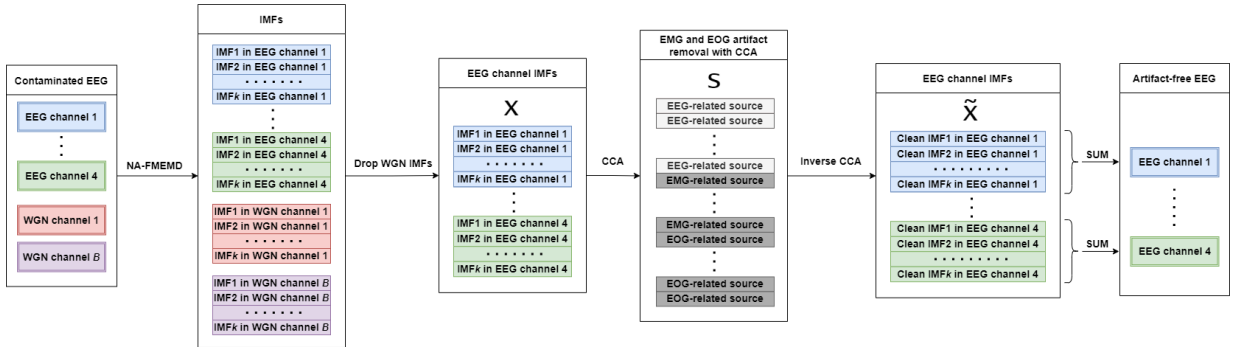


Figure 3: Flowchart for artifact removal using NA-FMEMD-CCA.

Decomposition of EEG using NA-FMEMD

FMEMD decomposes signals into multivariate IMFs, after which the artifact containing IMFs can be removed with CCA. Applying FMEMD directly to N EEG signals will lead to the existing problem of mode-mixing, where a single IMF contains multiple frequency bands, which is no difference from other EMD and MEMD methods. Adding M white Gaussian noise (WGN) signals with length T alleviates this problem, since the added WGN signals occupy a broad frequency range. This helps FMEMD decomposing the signals into modes which each carry only one frequency band [30]. The performance of NA-FMEMD is independent of the number of WGN channels, but too few channels of WGN might not alleviate the mode-mixing problem. On the other hand, excessive WGN channels are redundant and unnecessarily increase computational

load. The number of WGN channels is usually set on five as a balanced trade-off between performance and computational load [27]. FMEMD decomposes the dimensionality-increased $[N+M, T]$ data into K sets of IMFs, after which $K*N$ IMFs corresponding to WGN signals will be dropped. NA-FMEMD leaves a residual signal, which is the signal that cannot be decomposed further. The IMFs and the residual signal of one epoch are visualised in Figure 4a.

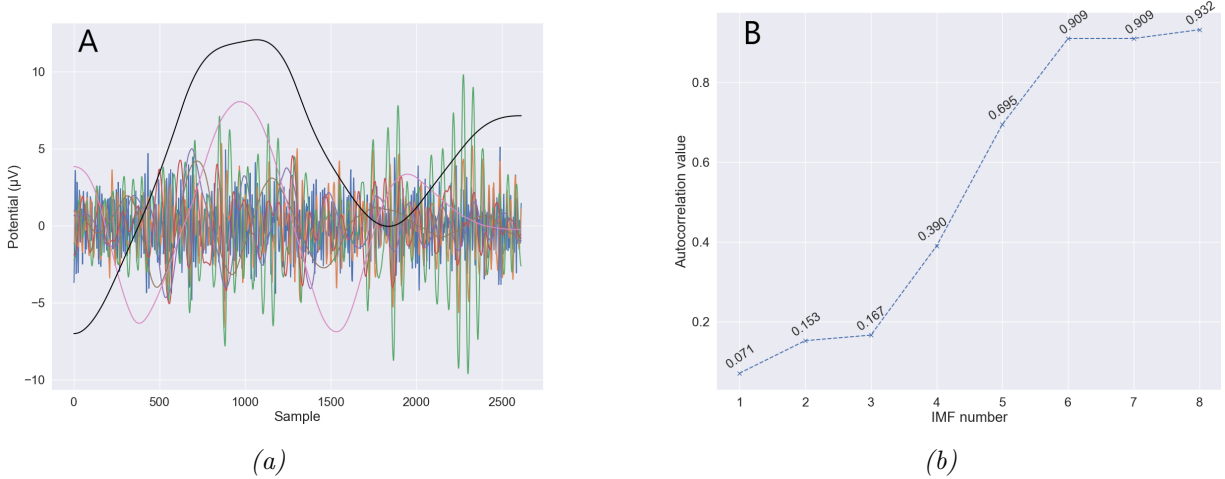


Figure 4: (a) Colored lines: IMFs belonging to one channel from one epoch. Black line: residual signal from NA-FMEMD. (b) Autocorrelation values corresponding to the underlying sources, calculated by CCA using IMFs from (a).

Unmixing into underlying sources using CCA

It is probable that the IMFs contain both brain activities and artifacts. This problem can be treated as a BSS problem, since there is very little knowledge about the mixing process, but there is actually some useful information known about the underlying sources. Namely, EMG artifacts have a relatively low autocorrelation and ocular artifacts have a relatively high autocorrelation in comparison with brain activity. CCA can calculate the underlying sources, which are uncorrelated with each other, but maximally autocorrelated with itself [27]. The IMF-containing matrix \mathbf{X} of size $[N, K, T]$ will be unmixed using the mixing matrix \mathbf{A} , obtained by CCA, into the underlying sources \mathbf{S} , according to equation 1.

Selecting and rejecting artifact-containing sources

Calculating the autocorrelation of every row in \mathbf{S} can give insight about which component contains artifacts, since the characteristics in terms of autocorrelation of EMG and ocular artifacts are known. For example, components with an autocorrelation <0.7685 could be treated as EMG artifacts and components with an autocorrelation >0.9975 could represent ocular artifacts. These components can be set to zero in the mixing matrix \mathbf{A} before the reconstruction of $\tilde{\mathbf{X}}$ [23]. Autocorrelation values corresponding to IMFs of one epoch are visualised in Figure 4b.

Reconstructing artifact-free EEG

Reconstruction of the IMFs can be done using the inverse of the mixing matrix \mathbf{A} . Finally, summing the IMFs corresponding to each EEG channel estimates the artifact free EEG signals.

Evaluation of artifact removal performance

The purpose of the artifact removal technique is removing artifacts while preserving nociceptive evoked brain activity. Frequently used evaluation methods like Relative Root Mean Squared Error (RRMSE) and Correlation Coefficient (CC) are not suitable to evaluate the proposed approach, as the real ground truth EEG signal is not available for real, non-simulated data. Methods used to evaluate the proposed artifact removal technique will be discussed in the following section.

EEG recordings from an experiment are used to evaluate the artifact removal performance and the preservation of nociceptive evoked brain activity. During the experiment, stimuli were applied to the participants while EEG was being recorded. The participants were instructed to hold a button and shortly release it if they perceived a stimulus. A data set consisting of these EEG recordings from previous research by Van den Berg *et al* is being used. In addition, brain activity during the experiment of four other participants is recorded.

Independent Component Analysis

Currently, Van den Berg *et al* [9] use independent component analysis (ICA) for artifact removal in 32+ channel EEG. ICA is a suitable BSS artifact removal technique for a multi-channel scenario, where independent sources \mathbf{S} can be recovered from highly correlated EEG \mathbf{X} in which they are linearly mixed with an unknown mixing matrix \mathbf{A} , shown in equation 1. ICA maximizes the statistical independence among output signals and minimizes the correlation between all variable pairs. In order to find a sufficient mixing matrix, ICA requires the number of underlying sources being smaller than the number of EEG channels [31]. ICA is mostly suitable for ocular artifact removal, but is sometimes used to remove other physiological artifacts. The major problem with artifact removal using ICA is that rejection of independent components (IC) normally requires manual intervention by selecting and removing artifact containing ICs, which can be done with help of information from, for example, power spectrum, scalp topography and signal visualisation. However, artifact containing IC selection and removal can be made automatic by labeling the ICs using some features such as canonical autocorrelation coefficient, kurtosis, skewness and fractal dimension (FD) [32]. Other limitations of ICA are computational complexity, which makes it unsuitable for real-time applications, and noise sensitivity [11].

$$\mathbf{X}(t) = \mathbf{A}\mathbf{S}(t) \tag{1}$$

Evaluation of nociceptive evoked brain activity preservation using deep learning

During the experiment, stimuli were applied to the participants while EEG was being recorded. The participants were instructed to release a button when they experienced a stimulus, which is called a Go/No-go (GN) task. Afterwards, a multilayer convolutional neural network was trained to perform a 2-Interval Forced Choice (2IFC) task, where it had to classify, between a pre- and post-stimulus interval, which of the two contained post-stimulus brain activity [9]. The tasks are visualized in Figure 5. The data set used for training and testing can be filtered by different artifact removal methods, for example ICA or NA-FMEMD-ICA, after which the deep neural networks (DNNs) can be trained. Comparing the DNNs performance can give an estimation of the relative competence of an artifact removal method in preserving nociceptive evoked brain activity while removing the artifacts.

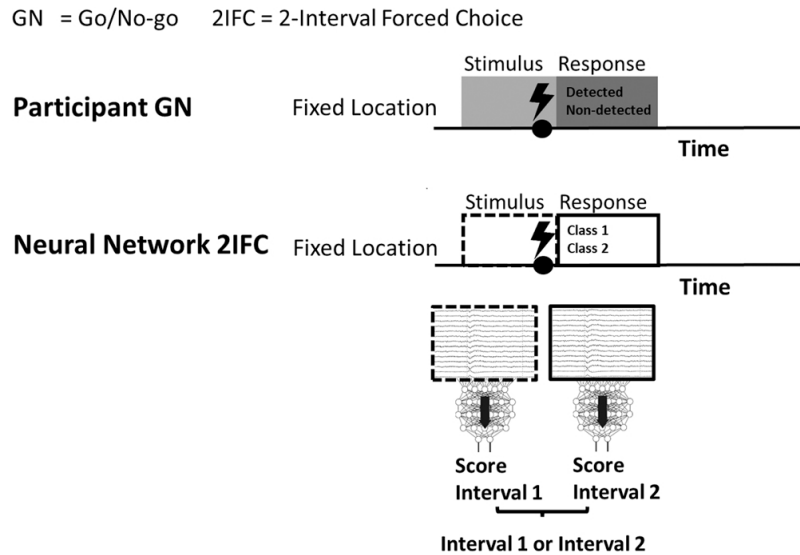


Figure 5: The Go/No-go task, in which the participant is asked to release a button when a stimulus was experienced. The neural network classifies in the 2IFC task which of the two given intervals contains post-stimulus brain activity [9].

Implications

The needed information about EEG artifacts and characteristics, artifact removal methods and evaluation techniques has been provided in this section. Knowledge about EEG artifact characteristics is necessary for recognising artifacts and comparing artifact removal method performances. Evaluation techniques will be used for evaluating artifact removal methods, since ground truth EEG is not available. NA-FMEMD-CCA is chosen as the most promising artifact removal method in a few-channel scenario, based on the fact that it has a low computational time and the ability to remove most types of artifacts. The performance of NA-FMEMD-CCA as an artifact removal technique in a few-channel scenario for nociceptive evoked brain activity recordings in compari-

son to the currently used method, will be studied further in this thesis. In addition, the effect of channel reduction on the quantity of nociceptive evoked brain activity content will be investigated as well.

4 Methods

Data acquisition

In total 4 healthy participants were included in this study. Exclusion criteria were implanted stimulation devices, pregnancy, usage of alcohol, drugs or analgesics within 24 hours before the start of the experiment, pain complaints at the time of the experiment or having a medical history of chronic pain.

Data set 1 (DS1)

An existing data set, recorded by Van den Berg *et al* at the University of Twente, is used to evaluate the performance of the artifact removal method. This data set consist of data of 24 healthy participants, from which 16 males and 8 females, in the age-range of 18 to 31. The used exclusion criteria, stimuli and procedure are similar to the exclusion criteria, stimuli and procedure I used to record new four channel EEG data.

The EEG was recorded on 128 Ag/AgCl electrodes with a common average reference, according to the international 10-5 system, with a sampling frequency of 1024 Hz using a REFA amplifier (TMSi B.V., Oldenzaal, The Netherlands). Electrode impedance was kept below 20 k Ω . This data set will be called DS1 in the following sections.

Data set 2 (DS2)

In total, EEG recordings of 4 male healthy participants were included in this data set, in the age-range of 21 to 47. All participants have signed a consent form before participating in the experiment.

The EEG was recorded on 4 Ag/AgCl electrodes with a common average reference, with a sampling frequency of 1024 Hz using a REFA amplifier (TMSi B.V., Oldenzaal, The Netherlands). The electrodes were located at T7, Cz, T8 and Fz, according to the international 10-5 system. Electrode impedance was kept below 20 k Ω . This data set will be called DS2 in the following sections.

Stimuli

Stimuli were generated by a constant current stimulator (NociTRACK AmbuStim, University of Twente, Enschede, The Netherlands). A custom made electrode, consisting of 5 inter-connected microneedles, applied the stimuli intra-epidermal to achieve activation of A δ -fibers. Stimulation using this electrode resulted in a prickling sensation. Three different settings with square-wave electrical current pulses were used during the experiment, namely:

1. Single 210 μ s pulse
2. Double 210 μ s pulse with an inter-pulse interval of 10 ms.
3. Double 210 μ s pulse with an inter-pulse interval of 40 ms.

Procedure

Participants were seated in a chair and received instructions to press and hold a button. For familiarization with the sensation of the stimuli, a series of stepwise (0.025 mA) increasing stimuli were applied until the participant released the button. The participants were instructed to release the button after a stimulus was perceived at least twice. After the familiarization, the initial detection threshold was approximated using the same series of stepwise increasing stimuli for which the participants were instructed to release the button when any sensation was perceived. Subsequently, 150 stimuli per stimulus type were applied to track nociceptive detection thresholds. As long as the button was pressed, stimuli were applied to the participant. A set of five stimuli with equidistant (0.025 mA) amplitudes around the initial detection threshold was used. A random stimulus from the set of five was applied. The participants were instructed to shortly release the button when a stimulus was experienced. A stimulus was identified as detected if the button was released within one second after the stimulus was applied. The amplitudes of the stimuli in the set were decreased by 0.025 mA if a stimulus was detected, and were increased by 0.025 mA if the stimulus was non-detected. This procedure was repeated for 450 stimuli in total, 150 stimuli for all three settings. Participants were instructed to fix their eyes on an image on the wall in front of them. They were asked to sit as still as possible and release the button before talking, in order to minimize the number of artifacts [33].

EEG pre-processing

The EEG data from DS1 was pre-processed twice using partly different pipelines. First, the EEG was resampled to 512 Hz in order to speed up computations. After the first step, the pipeline splits into two for artifact removal using ICA and NA-FMEMD-CCA. The EEG data in DS2 is pre-processed using the second, NA-FMEMD-CCA, pipeline.

- 1. ICA** Noisy or flat channels and segments in the EEG recordings were rejected manually. A copy of the data, used to calculate the underlying sources with ICA, was high-pass filtered using a cut-off frequency of 0.1 Hz to increase performance. The underlying components were approximated using ICA. Muscle, ocular and cardiac artifact containing components were manually rejected by altering the mixing matrix, based on scalp topography and visual signal-inspection. The mixing matrix was applied to the unfiltered data to obtain the cleaned EEG. Epochs were extracted in a range of -1.5s before stimulus up until 1.05s after the stimulus, using information from the stimulus trigger-channel. The channels belonging to the T7, Cz, T8 and Fz electrodes were selected from the EEG recordings. Finally, artifact containing epochs were manually removed using visual inspection and peak-to-peak limits, based on a histogram. EEG pre-processing using ICA is entirely done in Python using *MNE* [34].

2. NA-FMEMD-CCA The preselected channels, namely T7, Cz, T8 and Fz, were selected from the EEG recordings. Epochs were extracted in a range of -1.5s before stimulus up until 1.05s after the stimulus, using information from the stimulus trigger-channel. EMG and EOG artifacts were removed from the four channels using NA-FMEMD-CCA. The number of WGN channels was set to 5. The maximum number of IMFs per channel was set to 8 and the amount of epochs cleaned at once was 2, with an epoch length of 1307 samples. Artifacts were removed using autocorrelation thresholds, which values varied around a lower limit for muscle artifact removal and an upper limit for eye-blink artifact removal. Artifact removal using NA-FMEMD-CCA was done in Matlab using the *Fast and Adaptive Multivariate and Multidimensional EMD* toolbox [35] and the *ReMAE* toolbox [27][36]. The IMFs were reconstructed using the altered mixing-matrix, whereafter the sum of all IMFs per channel is taken to reconstruct the EEG signals. The NA-FMEMD residual of each channel is not used for reconstruction, since it mostly contains eye movement artifacts.

Performance evaluation

The proposed method must be evaluated for different autocorrelation thresholds. The recordings cleaned using NA-FMEMD-CCA are compared to the uncleaned recordings and the recordings filtered using ICA. Due to the absence of ground truth EEG, PSD, deep learning and visual inspection of the signal and the average EP are used to evaluate the performance of the proposed method. The three evaluation methods are applied on multiple NA-FMEMD-CCA threshold sets. The used thresholds for PSD and visual signal-inspection are showed in Table 3 and are based on results of previous research from Zhang *et al* [23]. The most promising threshold set is used to clean the data on which the deep neural network is trained. The most promising EOG artifact removal threshold is chosen using the requirement that it should not alter the details of the original signal, but should remove the majority of the EOG artifacts. The most promising EMG artifact removal threshold is chosen as the lowest threshold that removes most of the EMG artifacts, based on visual signal-inspection. In addition, the threshold should not affect frequencies lower than the beta rhythm, since that might change evoked potentials. The DNNs are trained and tested on data from DS1. In addition, the DNNs are also tested using uncleaned and NA-FMEMD-CCA-cleaned data from DS2. Finally, the average evoked potential at Cz is calculated and plotted for all recordings from DS1. This is done once for every variant of DS1 that the DNNs are trained on.

Table 3: Used threshold ranges for EMG artifact and ocular artifact removal.

EMG threshold	Ocular threshold
0 - 0.3	0.9955 - 1.0
0 - 0.5	0.9975 - 1.0
0 - 0.7	0.9995 - 1.0
0 - 0.9	1.0 - 1.0

Power spectral density

EEG recording number 5 from DS1 was cleaned using either NA-FMEMD-CCA or ICA. The power spectral density, using Welch’s method, of the uncleaned EEG recording, the ICA-filtered EEG recording and the NA-FMEMD-CCA-filtered EEG recording is calculated for each of the four channels.

Visual signal-inspection

An eye movement artifact containing epoch and an eye-blink artifact containing epoch from recording number 5 of DS1 was selected and cleaned using either NA-FMEMD-CCA or ICA. The cleaned epochs and the uncleaned epochs are plotted and are visually inspected to determine the performance of the artifact removal technique. This part is not done for an EMG artifact, since proper judgement of EMG artifact removal performance is impossible using visual signal-inspection as the ground truth is not available.

Average evoked potential

The average evoked potential is calculated by averaging all epochs from the entire data set DS1. This is done for uncleaned data, ICA-cleaned data, NA-FMEMD-CCA-cleaned data, data from which only EMG artifacts were removed using NA-FMEMD-CCA and data from which only EOG artifacts were removed using NA-FMEMD-CCA.

Deep neural network

An adapted version of EEGnet [37] was trained to perform a 2IFC task. In total, 10 DNNs were trained and validated. One trained and validated using uncleaned data, one using ICA-cleaned data, one on a data set cleaned using NA-FMEMD-CCA, one trained on a data set from which only EMG artifacts were removed using NA-FMEMD-CCA and one trained on a data set from which only EOG artifacts were removed using NA-FMEMD-CCA. All DNNs are trained and validated twice on different input lengths, namely 0.5s and 0.1s. This is done to avoid overfitting the DNN on eye-blink artifacts, since some participants might blink when they perceived a stimulus. The epochs belonging to detected stimuli were used to train and validate the DNNs. The epochs were split into pre-stimulus and post-stimulus activity pre- and post-stimulus ranges, namely (-1.5s – -1.0s ; 0.05s – 1.05s) and (-1.0s – -0.5s ; 0.05s – 0.55s). All epochs were standardized to increase performance. A total of 10120 intervals was used for training and testing the DNNs for NA-FMEMD-CCA and unfiltered data. 8586 intervals were used for training and testing the DNN which represents ICA. Half of the intervals was pre-stimulus and half was post-stimulus. On average, 16.7 % of the total epochs was used as test set. The used network architecture is shown in Table 4. Training was done with 15 epochs, a mini-batch size of 256, a gradient threshold of 2 and an initial learning rate of 0.1 which decreased with a factor 0.2 every 3 epochs. The accuracy of the DNNs was evaluated using 6-fold cross-validation where epochs of 4 EEG recordings were used for testing and epochs of 20 non-overlapping EEG recordings from

different participants were used for training. A total of 1628 intervals was used to test the DNNs on 4-channel EEG data from DS2.

Table 4: Architecture of the used neural network, an adapted version of EEGnet [37].

Layer (type)	Output Shape	Param #	Filter #	Activation
Input	(4, 512, 1)	0		
Conv2D	(4, 512, 8)	2048	8	Linear
BatchNorm	(4, 512, 8)	32		
Depthwise Conv2D	(1, 512, 16)	64	16	Linear
BatchNorm	(1, 512, 16)	64		
Activation	(1, 512, 16)	0		ELU
AveragePooling2D	(1, 128, 16)	0		
Dropout	(1, 128, 16)	0		
SeparableConv2D	(1, 128, 16)	512	16	Linear
BatchNormalization	(1, 128, 16)	64		
Activation	(1, 128, 16)	0		ELU
AveragePooling2D	(1, 16, 16)	0		
Dropout	(1, 16, 16)	0		
Flatten	256	0		
Dense	2	514		Softmax

5 Results

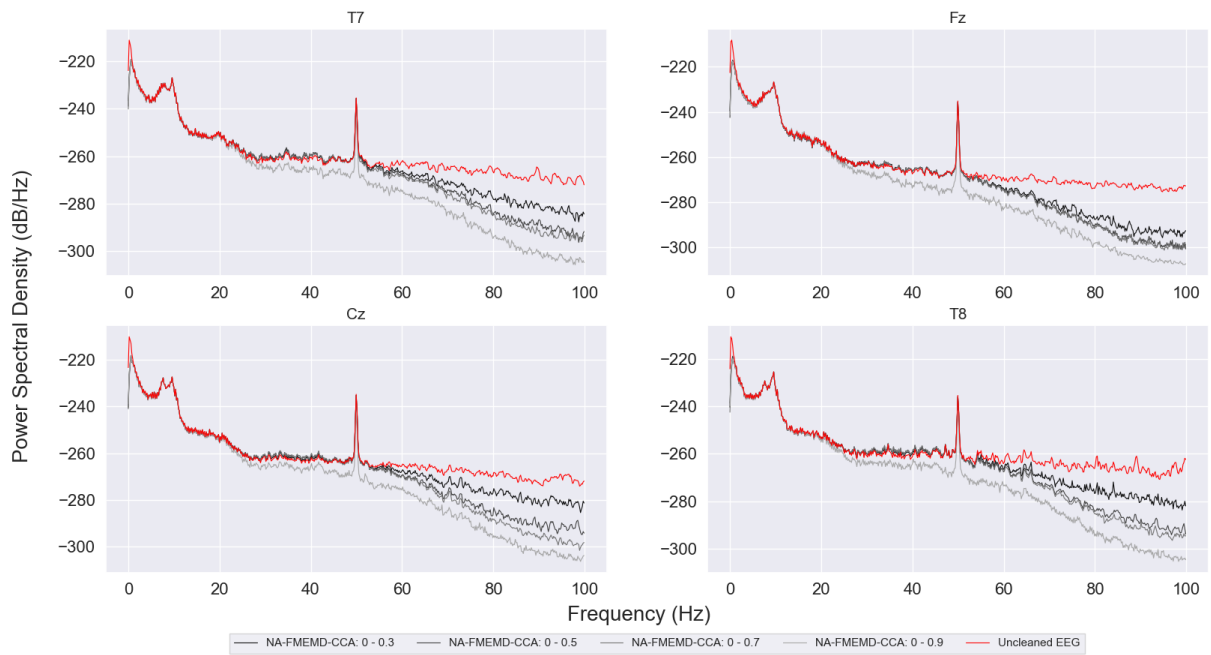
Qualitative comparison of artifact removal performance

ICA and NA-FMEMD-CCA were applied on one EEG recording for a qualitative comparison using power spectral density plots and visual inspection of artifacts, the entire signal and average evoked potentials. The recording was cleaned several times using different thresholds in order to investigate the artifact removal performance for different thresholds.

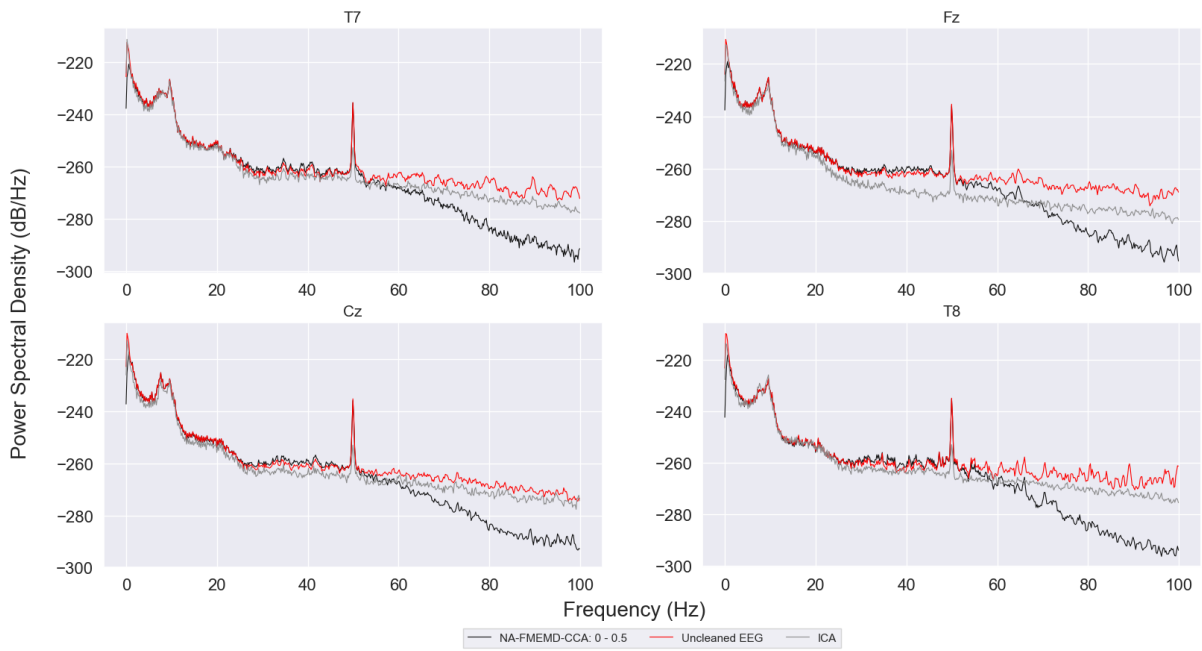
Muscle artifacts

Figure 6a shows the PSD of an EEG recording cleaned using different NA-FMEMD-CCA threshold sets. Lines corresponding to the threshold sets 0 - 0.3, 0 - 0.5 and 0 - 0.7 show a decrease in power at frequencies higher than 50 Hz. Also, the three lines show a small but notable increase in power at frequencies higher than 50 Hz. Also, the three lines show a small but notable increase in power at 25 - 45 Hz. Frequencies lower than 25 Hz seem unaffected in the three lines. The line corresponding to the threshold set 0 - 0.9 decreases in power at frequencies higher than 25 Hz and shows a decrease at frequencies lower than 3 Hz. All lines in all channels display a greater decrease in power at higher frequencies. Higher thresholds show a greater decrease in power at increasing frequencies. Threshold sets 0 - 0.5, 0 - 0.7 and 0 - 0.9 seem to remove most EMG from the EEG signal.

Figure 6b shows the PSD of the EEG recording cleaned using ICA and the most promising EMG artifact removal threshold set, according to 6a. ICA decreases power of the signal at most frequencies. The decrease is the greatest in channel Fz. NA-FMEMD-CCA shows a slight decrease in power at frequencies lower than 3 Hz, a small increase in power between 25 Hz and 45 Hz and an increasing decrease of power in frequencies higher than 50 Hz. Frequencies between 3 and 25 Hz are unaffected. The decrease of power at higher frequencies is greater in the NA-FMEMD-CCA line compared to the ICA line.



(a)



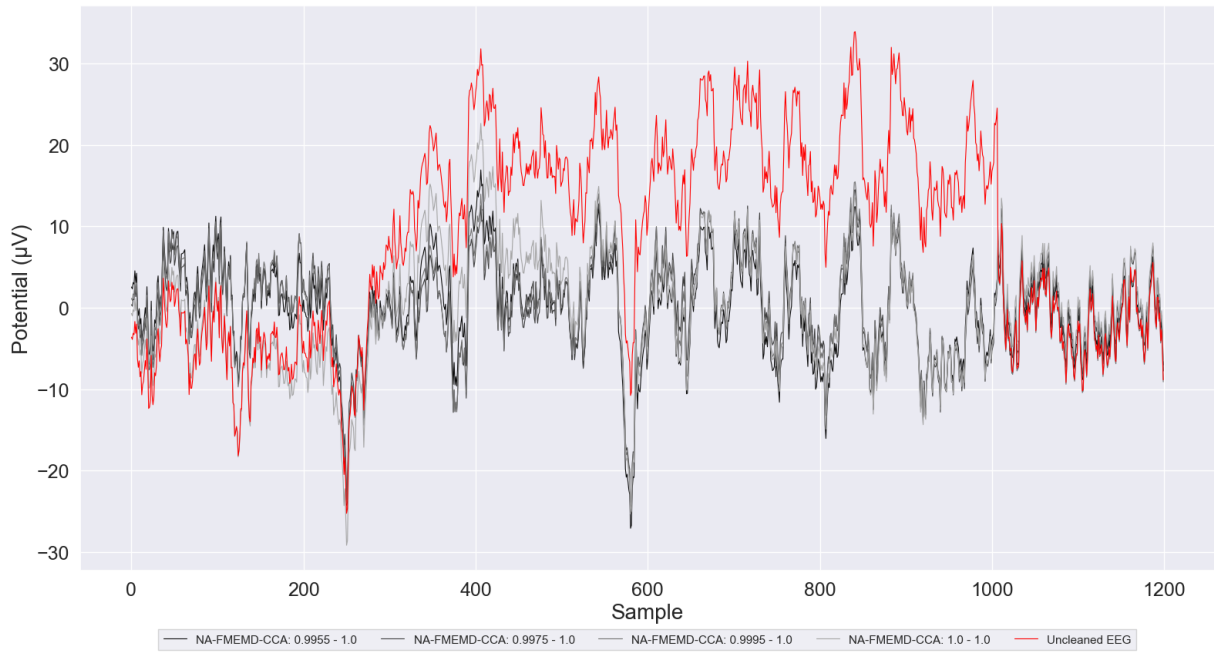
(b)

Figure 6: (a) PSD of uncleaned EEG and NA-FMEMD-CCA-cleaned EEG, using four different EMG threshold sets. (b) PSD of uncleaned EEG, ICA-cleaned EEG and NA-FMEMD-CCA-cleaned EEG using the best EMG threshold set.

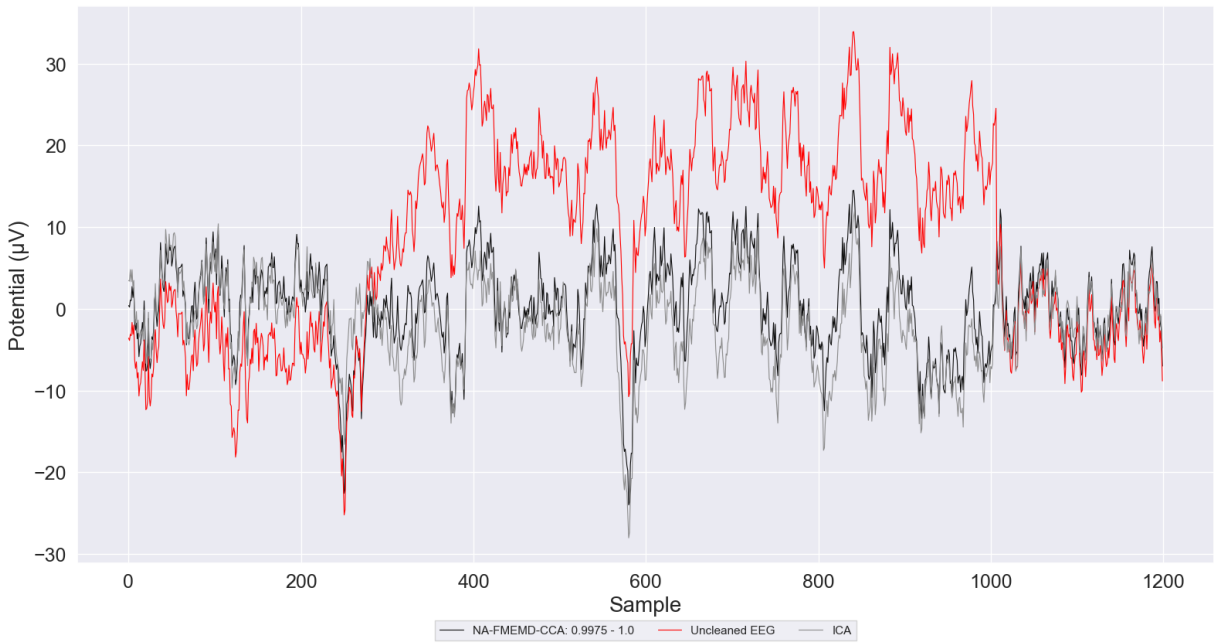
Ocular artifacts

Figure 7a displays the eye movement artifact containing EEG segment in red and several cleaned EEG segments using different threshold values. The darker lines are cleaned using lower thresholds. Consequently, the darker lines consist of less components than the lighter lines. All lines contain the characteristics of the red line, but without (part of) the eye movement artifact. The lightest colored line is slightly higher between samples 300 and 500 compared to the other cleaned segments and did not remove the artifact entirely. Figure 8a displays an eye-blink artifact containing EEG segment in red and several cleaned EEG segments using different threshold values. The thresholds 0.9995 - 1.0 and 1.0 - 1.0 do not remove the eye-blink artifact, while the lower thresholds do remove the artifact. The line corresponding to 0.9955 - 1.0 does alter the details of the EEG signal, for example between sample numbers 180 and 200. Inspection of the entire EEG recording showed that the threshold set 1.0 - 1.0 only removed (parts of) eye movement artifacts, while 0.9995 - 1.0 removed eye movement artifacts entirely and some eye-blink artifacts. The threshold set 0.9975 - 1.0 removed all eye movement artifacts and the majority of the eye-blink artifacts, which is similar ocular artifact removal performance to ICA. However, the threshold range 0.9975 - 1.0 is unable to entirely remove very intense spiking eye-blink artifacts and clean epochs that contain multiple eye-blink artifacts. Figure 9a shows the PSD corresponding to the entire EEG recording, which was cleaned using the same thresholds as showed in Figure 7a and Figure 8a. All lines show a slight decrease in power at frequencies lower than 10 Hz. The darker the line, the lower the threshold and the greater the decrease. Higher frequencies seem unaffected by ocular removal thresholds.

Figure 7b shows the segment cleaned by the most promising ocular artifact removal threshold for NA-FMEMD-CCA, ICA and the uncleaned segment for comparison. Both ICA and NA-FMEMD-CCA follow the uncleaned signal at the beginning and the end of the segment, and are able to lower the signal while containing the details from the red line. Figure 8b shows the eye-blink artifact containing segment cleaned by either ICA and NA-FMEMD-CCA using the same threshold as used in Figure 7b. ICA slightly alters the details in the signal, but does not remove the artifact, while NA-FMEMD-CCA removes the entire eye-blink artifact while keeping all the details of the red line. Figure 9b shows the PSD corresponding to the entire EEG recording, cleaned using the same cleaning methods as in Figure 7b and Figure 8b. ICA shows significant decrease in power at frequencies higher than 15 Hz, while NA-FMEMD-CCA only shows a decrease in power at frequencies lower than 10 Hz.



(a)

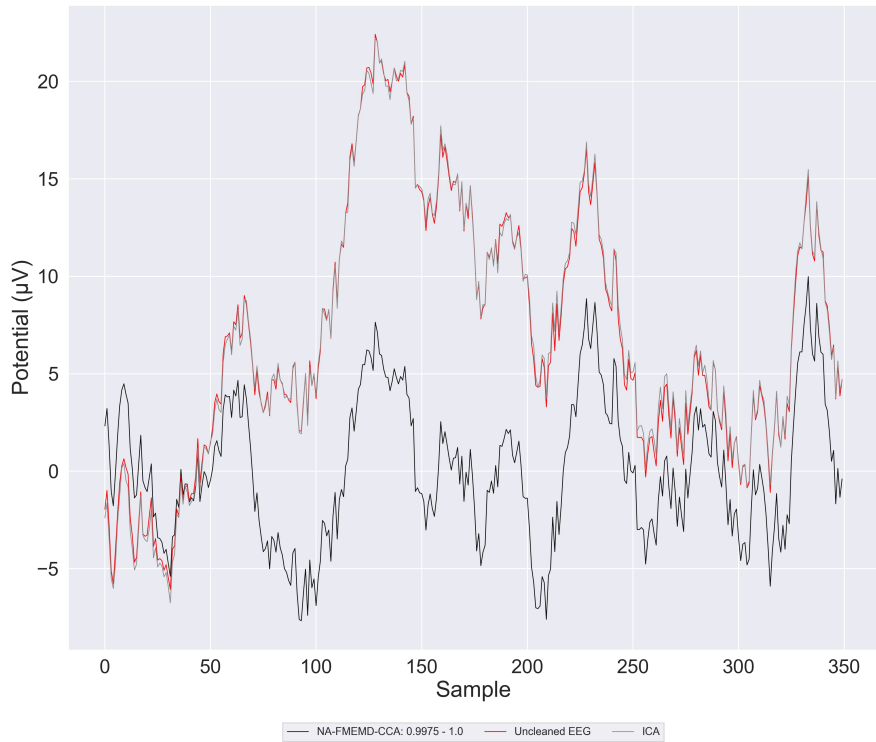


(b)

Figure 7: Eye movement artifact containing EEG segment at T8, cleaned using: (a) NA-FMEMD-CCA using four different EOG threshold sets. (b) either ICA or NA-FMEMD-CCA using the most promising EOG threshold set.

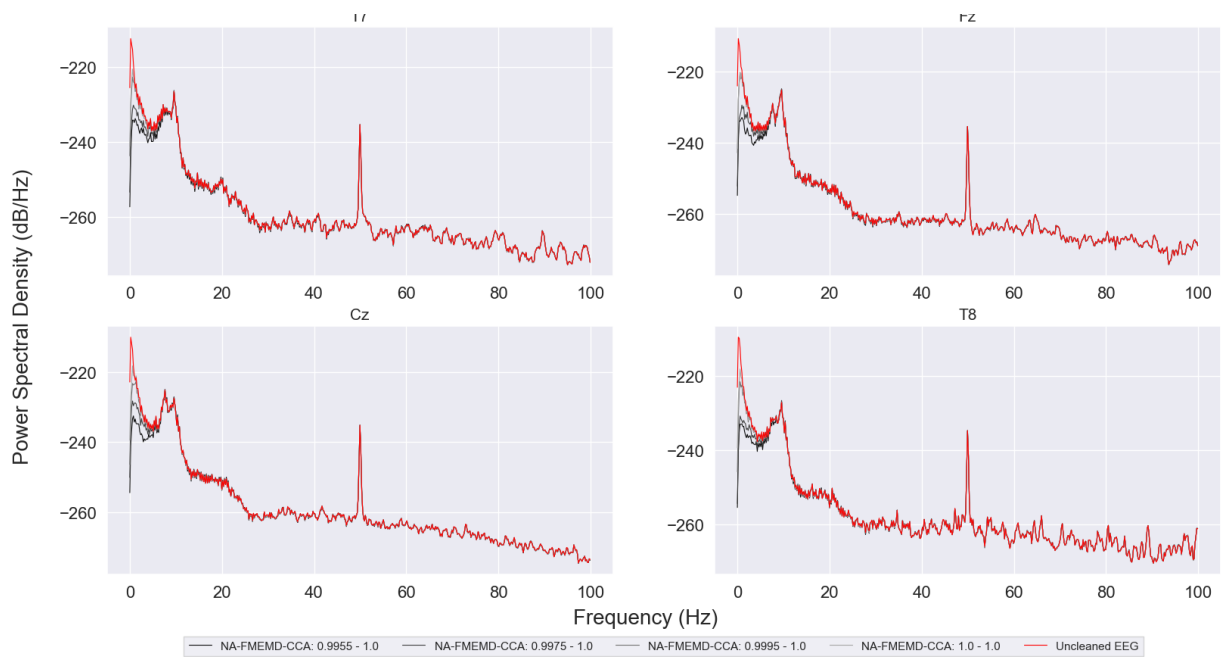


(a)

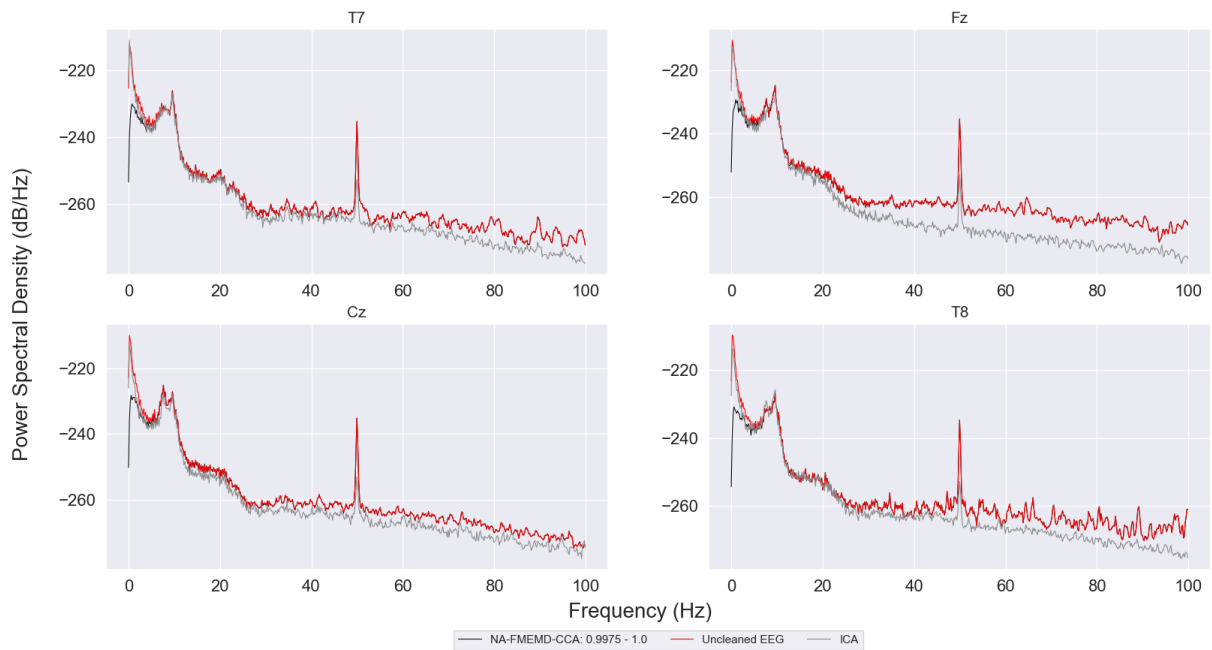


(b)

Figure 8: Eye-blink artifact containing EEG segment at Cz, cleaned using: (a) NA-FMEMD-CCA using four different EOG threshold sets. (b) either ICA or NA-FMEMD-CCA using the most promising EOG threshold set.



(a)



(b)

Figure 9: (a) PSD of uncleaned EEG and NA-FMEMD-CCA-cleaned EEG, using four different EOG threshold sets. (b) PSD of uncleaned EEG, ICA-cleaned EEG and NA-FMEMD-CCA-cleaned EEG using the best EOG threshold set.

Evoked potential

Figure 10 shows the average evoked potential for different cleaning methods. The red line represents the EP from the uncleaned data and the other lines represent EPs from data cleaned using either ICA or NA-FMEMD-CCA. All EPs show a clear N1 and P1 peak. The maximum amplitude of the P1 peak of the uncleaned data EP is higher than P1 peaks in all other EPs. The ICA-cleaned EP and the NA-FMEMD-CCA-cleaned EP using the EMG artifact threshold (0 - 0.5; 1.0 - 1.0) show a similar maximum amplitude of the P1 peak. The cleaned data using NA-FMEMD-CCA threshold sets (0 - 0.5; 0.9975 - 1.0) and (0 - 0; 0.9975 - 1.0) show an almost equal EP, but the maximum amplitude of the P1 peak is lower than the maximum amplitudes of the P1 peaks in the other EPs.

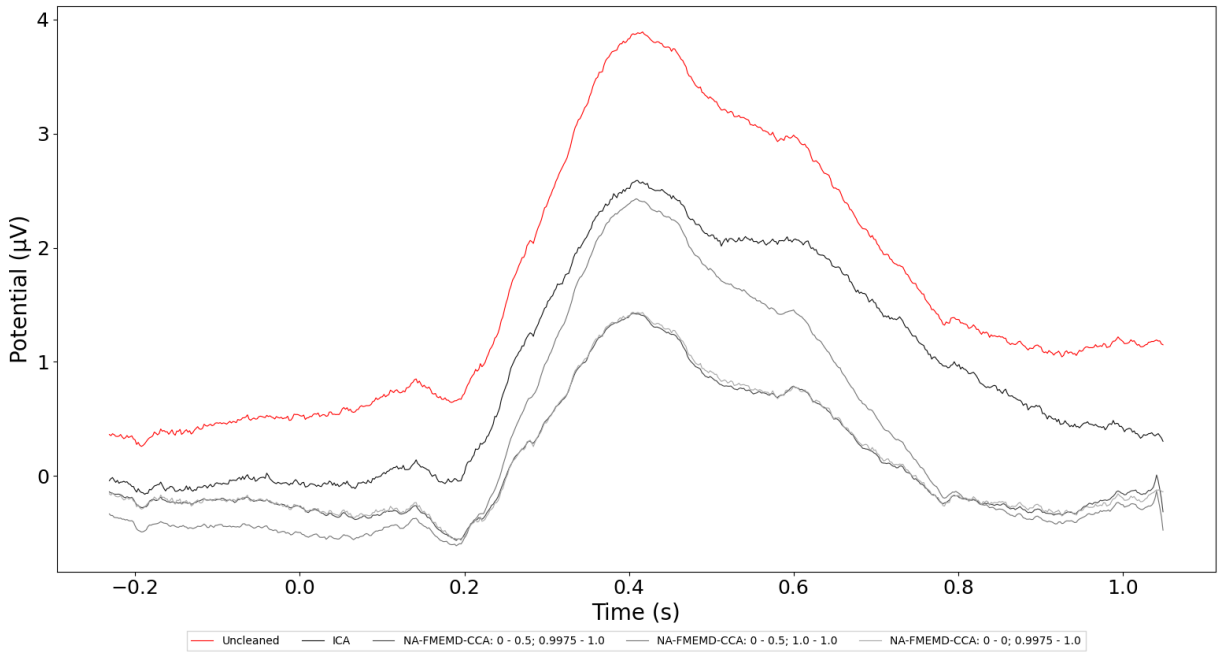


Figure 10: Average evoked potential at Cz for different cleaning methods. The red line represents the average EP from the uncleaned data set DS1. The grey-colored lines are average EPs calculated from cleaned versions of DS1.

Quantitative comparison of EEG preservation

For this section, the entire DS1 data set is cleaned using either ICA or NA-FMEMD-CCA, with the previous determined thresholds. Deep neural networks are trained on the uncleaned data set and the two cleaned data sets. The four four-channel EEG recordings are cleaned using NA-FMEMD-CCA and used to evaluate trained neural networks.

Deep neural network

The ten DNNs (0.5s input: uncleaned, ICA-cleaned, 3x NA-FMEMD-CCA-cleaned ; 1s input: uncleaned, ICA-cleaned, 3x NA-FMEMD-CCA-cleaned) are validated using 6-fold cross-validation. The results of the cross-validation are visualized in Table 5 and Table 6. Table 5 shows the performance of the DNNs with a 1s input. The DNNs trained on uncleaned data (0.778 ± 0.032) and ICA-cleaned data (0.771 ± 0.019) have a similar average accuracy, while the NA-FMEMD-CCA DNN has a three percent point lower average accuracy (0.744 ± 0.013). The best performing DNN trained on NA-FMEMD-CCA-cleaned data has an accuracy of 0.75. The DNN trained on data from which only EMG artifacts were (partly) removed performs significantly better (0.766 ± 0.038) than the DNNs that were trained on data without (most of the) EOG artifacts. This DNN shows equal performance to the DNNs trained on uncleaned data and ICA-cleaned data. Table 6 shows the performance of the DNNs with a 0.5s input. Again, the performance of the two DNNs trained on EOG artifact free data, cleaned using NA-FMEMD-CCA, is worse compared to the other three DNNs. The DNN trained on data cleaned using NA-FMEMD-CCA with EMG thresholds performs almost as good as the DNNs trained on uncleaned data and ICA-cleaned data. However, all DNNs show a significant decrease in accuracy compared to the 1s input DNNs.

Table 5: 6-fold cross-validation of 1s input DNN, trained on uncleaned data, ICA-cleaned data and NA-FMEMD-CCA-cleaned data. Cleaning using NA-FMEMD-CCA is separately done with three sets of thresholds: (0 - 0.5; 0.9975 - 1.0), EMG artifact removal threshold (0 - 0.5; 1.0 - 1.0) and EOG artifact removal threshold (0 - 0; 0.9975 - 1.0).

Cleaning method	Fold	Trng. intv. #	Test intv. #	Trng. Loss	Trng. Acc.	Val. Loss	Val. Acc.
Uncleaned	1	8444	1676	0.455	0.789	0.427	0.806
	2	8350	1770	0.447	0.795	0.470	0.768
	3	8432	1688	0.435	0.800	0.499	0.759
	4	8350	1770	0.450	0.793	0.439	0.807
	5	8510	1610	0.441	0.801	0.434	0.808
	6	8514	1606	0.434	0.805	0.570	0.723
	Average (± Std.)	8433	1687	0.444 ± 0.008	0.797 ± 0.005	0.437 ± 0.050	0.778 ± 0.032
ICA	1	7268	1318	0.448	0.793	0.466	0.779
	2	7120	1466	0.441	0.796	0.501	0.750
	3	7056	1530	0.423	0.803	0.545	0.746
	4	7018	1568	0.454	0.793	0.443	0.802
	5	7208	1378	0.444	0.796	0.471	0.778
	6	7260	1326	0.451	0.792	0.476	0.772
	Average (± Std.)	7155	1431	0.444 ± 0.010	0.796 ± 0.004	0.484 ± 0.032	0.771 ± 0.019
NA-FMEMD-CCA (0 - 0.5; 0.9975 - 1.0)	1	8444	1676	0.509	0.760	0.513	0.747
	2	8350	1770	0.503	0.760	0.526	0.755
	3	8432	1688	0.509	0.757	0.545	0.725
	4	8350	1770	0.500	0.760	0.515	0.752
	5	8510	1610	0.511	0.750	0.493	0.759
	6	8514	1606	0.500	0.756	0.543	0.729
	Average (± Std.)	8433	1687	0.505 ± 0.0	0.757 ± 0.004	0.522 ± 0.018	0.744 ± 0.013
NA-FMEMD-CCA (0 - 0.5; 1.0 - 1.0)	1	8444	1676	0.473	0.771	0.450	0.794
	2	8350	1770	0.458	0.787	0.470	0.777
	3	8432	1688	0.464	0.782	0.523	0.742
	4	8350	1770	0.467	0.786	0.452	0.792
	5	8510	1610	0.467	0.781	0.445	0.799
	6	8514	1606	0.461	0.787	0.622	0.691
	Average (± Std.)	8433	1687	0.465 ± 0.005	0.782 ± 0.005	0.494 ± 0.063	0.766 ± 0.038
NA-FMEMD-CCA (0 - 0; 0.9975 - 1.0)	1	8444	1676	0.516	0.750	0.542	0.729
	2	8350	1770	0.520	0.745	0.537	0.724
	3	8432	1688	0.503	0.756	0.538	0.735
	4	8350	1770	0.513	0.752	0.544	0.733
	5	8510	1610	0.518	0.746	0.484	0.770
	6	8514	1606	0.483	0.769	0.542	0.741
	Average (± Std.)	8433	1687	0.509 ± 0.013	0.753 ± 0.008	0.531 ± 0.021	0.739 ± 0.014

Table 6: 6-fold cross-validation of 0.5s input DNN, trained on uncleaned data, ICA-cleaned data and NA-FMEMD-CCA-cleaned data. Cleaning using NA-FMEMD-CCA is separately done with three sets of thresholds: (0 - 0.5; 0.9975 - 1.0), EMG artifact removal threshold (0 - 0.5; 1.0 - 1.0) and EOG artifact removal threshold (0 - 0; 0.9975 - 1.0).

Cleaning method	Fold	Trng. intv. #	Test intv. #	Trng. Loss	Trng. Acc.	Val. Loss	Val. Acc.
Uncleaned	1	8444	1676	0,541	0,736	0,539	0,723
	2	8350	1770	0,538	0,736	0,551	0,723
	3	8432	1688	0,538	0,731	0,530	0,742
	4	8350	1770	0,526	0,746	0,548	0,722
	5	8510	1610	0,532	0,732	0,534	0,737
	6	8514	1606	0,526	0,775	0,571	0,722
	Average (± Std.)	8433	1687	0,533 ± 0,006	0,743 ± 0,015	0,546 ± 0,015	0,728 ± 0,008
ICA	1	7268	1318	0,509	0,753	0,536	0,733
	2	7120	1466	0,512	0,751	0,579	0,696
	3	7056	1530	0,525	0,741	0,508	0,758
	4	7018	1568	0,509	0,748	0,537	0,730
	5	7208	1378	0,500	0,759	0,503	0,768
	6	7260	1326	0,517	0,754	0,521	0,747
	Average (± Std.)	7155	1431	0,512 ± 0,008	0,751 ± 0,005	0,530 ± 0,025	0,738 ± 0,025
NA-FMEMD-CCA (0 - 0.5; 0.9975 - 1.0)	1	8444	1676	0,577	0,705	0,615	0,657
	2	8350	1770	0,580	0,697	0,580	0,680
	3	8432	1688	0,585	0,690	0,588	0,689
	4	8350	1770	0,593	0,690	0,597	0,669
	5	8510	1610	0,595	0,688	0,602	0,685
	6	8514	1606	0,577	0,697	0,590	0,696
	Average (± Std.)	8433	1687	0,585 ± 0,007	0,694 ± 0,006	0,595 ± 0,011	0,679 ± 0,013
NA-FMEMD-CCA (0 - 0.5; 1.0 - 1.0)	1	8444	1676	0,543	0,729	0,537	0,737
	2	8350	1770	0,540	0,736	0,554	0,712
	3	8432	1688	0,530	0,742	0,537	0,730
	4	8350	1770	0,540	0,737	0,557	0,707
	5	8510	1610	0,543	0,728	0,522	0,750
	6	8514	1606	0,531	0,746	0,587	0,711
	Average (± Std.)	8433	1687	0,538 ± 0,005	0,736 ± 0,006	0,549 ± 0,020	0,724 ± 0,015
NA-FMEMD-CCA (0 - 0; 0.9975 - 1.0)	1	8444	1676	0,573	0,705	0,601	0,677
	2	8350	1770	0,581	0,695	0,572	0,698
	3	8432	1688	0,591	0,687	0,585	0,691
	4	8350	1770	0,579	0,701	0,591	0,680
	5	8510	1610	0,588	0,693	0,581	0,688
	6	8514	1606	0,589	0,688	0,611	0,668
	Average (± Std.)	8433	1687	0,583 ± 0,006	0,695 ± 0,006	0,590 ± 0,012	0,684 ± 0,009

Proof of principle

Segments of 1s of the 4-channel EEG recordings were classified using the best performing DNNs, trained on uncleaned and NA-FMEMD-CCA-cleaned data using both EMG and EOG thresholds. The network classified uncleaned pre-stimulus and post-stimulus segments with an accuracy of 0.72. The classification accuracy of the DNN on cleaned data is 0.66. The network performed better on cleaned pre-stimulus segments than on cleaned post-stimulus segments. The other network performed better on uncleaned post-stimulus segments.

6 Discussion

The current experiment setup for measuring nociceptive evoked brain activity is not yet suitable for a clinical setting, partly caused by the required time for applying an 32+ channel EEG cap. In this work, I proposed an automated method to remove EOG and EMG artifacts from EEG recordings using only four EEG channels, in order to make EEG more suitable for diagnosis support in a clinical setting.

The performance of the proposed artifact removal method, NA-FMEMD-CCA, depends entirely on the chosen autocorrelation threshold values. Larger threshold ranges are more suitable for removing EOG and EMG artifacts, but also appear to affect brain activity content. The final chosen threshold set, (0 - 0.5; 0.9975 - 1.0), removes the majority of the artifacts, but also affects the EEG content, which can be concluded from the performance of the DNNs. Perfectly cleaned data should at least perform as good as uncleaned data, since the deep neural networks should be able ignore most artifacts. A significant decrease in performance of the DNN trained on NA-FMEMD-CCA-cleaned data, compared to the DNN trained on uncleaned data, illustrates loss of brain activity content. The DNN trained on ICA-cleaned data showed a similar average accuracy as the uncleaned data DNN, 0.771 and 0.778 respectively, which confirms the preservation of most nociceptive evoked EEG content. The DNN trained on NA-FMEMD-CCA-cleaned data had an average accuracy of 0.744 during 6-fold cross-validation and a disappointing accuracy of 0.661 on the 4-channel EEG recordings. The DNN trained on data from which only EMG artifacts are removed using NA-FMEMD-CCA performs significantly better than the DNN trained on data from which EOG artifacts are cleaned using NA-FMEMD-CCA, as can be seen in Table 5.

From these results it is clear that the EOG threshold is mostly responsible for the loss of important nociceptive evoked brain activity content. However, the DNN trained on EMG artifact cleaned data also shows a small decrease in accuracy, compared to the DNNs trained on uncleaned data and ICA-cleaned data. Inspection of the average EPs in Figure 10 confirm these findings. The data cleaned using the EOG threshold contain EPs with a significant lower amplitude P1 peak, compared to the EPs in the data cleaned using the EMG threshold. This points out that the use of the EOG threshold affects the EP.

Difference in performance between the DNNs could be caused by the fact that the DNN fitted on eye-blink artifacts, since some participants might blink after they perceived a stimulus. However, the DNNs with an 0.5s input, which does not include the eye-blink, also show significant differences in accuracy between uncleaned data and NA-FMEMD-CCA-cleaned data, which again illustrates loss of brain activity content. Loss of EEG content is probably mainly caused by the EOG threshold range, since this threshold affects the frequencies at which both EOG and the evoked potentials are present, while it is being uncertain if the thresholds only removes EOG related components. Moreover, components could contain both EEG and EOG content, which makes it harder to clean the signal. Higher thresholds might preserve EEG, but decrease the per-

formance of EOG artifact removal. An interesting insight is that the EMG threshold 0 - 0.3 does not remove any EMG artifacts, but it does remove a significant amount of signal at frequencies higher than 50 Hz, according to the PSD plot in Figure 6a. It might be possible that components with autocorrelation values lower than 0.3 contain high frequency EEG content, which will be removed when a threshold higher than 0.3 is being used. This might explain the small performance loss caused by the EMG threshold.

The lower accuracy of the DNN on 4-channel EEG recordings could also be explained by the fact that the DNN is trained on data of 32-channel EEG recordings and tested on data of 4-channel EEG recordings. The use of common average reference introduces a difference between the two types of recordings, which complicates predictions for the DNN.

When comparing the results of artifact removal performance to the study of Zhang *et al* [23], it must be pointed out that the optimal EMG threshold I found is lower than the threshold stated in their study, 0.5 and 0.7685 respectively. However, the found EOG thresholds and corresponding performance are equal. Contrary to the findings of Zhang *et al*, the EEG content was affected by both EOG threshold and EMG threshold. The difference in performance could be explained by the fact that the researchers only investigated up to 50 Hz. The signal, cleaned using the EMG threshold I chose, shows decrease of power at frequencies higher than 50 Hz. The researchers might have had the same results but did not investigate those frequencies, which makes comparison difficult. The difference in performance caused by the EOG threshold could be explained by the fact that Zhang *et al* did not investigate artifact removal for nociceptive evoked brain activity content. Moreover, I used other evaluation methods than Zhang *et al*, which makes comparison difficult. In general, performance difference could be explained by the used sample frequency, since the researchers used a sample frequency of 256 Hz, compared to 512 Hz sample frequency used in this thesis.

Besides loss of brain activity content due to artifact removal, loss of important information could also be caused by reduction of the number of used EEG channels. Van den Berg *et al* [9] trained a DNN on ICA-cleaned 32-channel EEG data to perform a 2IFC task. Their DNN performed the task with an average accuracy of 0.75 during 10-fold cross-validation and an accuracy of 0.82 on the test set. The DNN trained on ICA-cleaned 4-channel EEG data showed an average accuracy of 0.77, which is surprisingly higher than using 32 channels. This could point out that the four preselected channels contain most of the important nociceptive evoked brain activity content. However, one possible explanation for the difference in performance could be the size of the test set, which was three times smaller in the cross-validation in this thesis. The smaller test set could result in less accurate validations. However, the other study used a training set almost five times larger than the data set I used in this thesis, which is normally in deep learning a huge advantage in terms of performance. The type of data set also influences the performance. Van den Berg *et al* [9] used EEG recordings from participants in a much larger age range compared to the data set I used, which certainly affects the quality of the recordings and thus might affect the performance.

Another explanation of the performance difference could be the manual removal of bad epochs and channels. Van den Berg *et al* [9] did not remove bad epochs or channels from their data set, which makes artifact removal harder for ICA and thus results in training the DNN on a less cleaned data set. Moreover, since I did not use a clear definition of 'bad epoch', I might have manually removed too many artifact containing epochs, making artifact removal more easy for ICA and thus training the DNN on an easier data set.

Limitations

There are at least three potential limitations concerning the results of this study. A first limitation concerns subjective judgement of removed artifacts. Misjudgement of artifact removal performance was possible, since artifact removal was not objectively measured as ground truth EEG was not available. This could have resulted in incorrect chosen thresholds. A second potential limitation is that the DNNs were trained using 4-channel EEG data from 32-channel recordings. EEG data recorded using 4-channel EEG differs from 32-channel EEG recordings, since common average reference is used. This makes comparison between 4-channel EEG and 32-channel EEG more difficult. The final limitation is that the performance of only a small set of thresholds was investigated, due to time constraints. Performance of the proposed artifact removal method could be increased by using a more specific threshold set.

7 Conclusion

EEG offers interesting opportunities for assessing sensory deficits, but requires simplification for widescale use in a clinical context. In this work, I showed that the number of EEG channels can be reduced to four, while keeping most of the nociceptive evoked brain activity content. However, the proposed artifact removal method NA-FMEMD-CCA loses important nociceptive evoked brain activity content and is unable to remove some eye-blink and EMG artifacts. Better tuned parameters might improve the performance of NA-FMEMD-CCA, which requires further investigation. Channel reduction significantly shortens the time required for applying an EEG cap, which brings the use of nociceptive EEG recordings one step closer to the clinic.

Recommendations for future research

Future research should further investigate threshold values in order to preserve more important nociceptive evoked brain activity content after artifact removal. In addition, it is important that future research expands the four channel EEG data set, since it will support more specific analysis for future research on this topic. Finally, it should be investigated which electrodepositions should be used to record the most nociceptive evoked brain activity content.

Acknowledgments

First of all, I would like to express my gratitude to my daily supervisor Boudewijn van den Berg, who guided me throughout this thesis. Furthermore, I would like to thank Jan Buitenweg and Jeroen Rouwkema for their role as committee members. Finally, I would like to thank the Biomedical Signals and Systems group at the University of Twente for their hospitality and support while I was working on this thesis.

References

1. Breivik H, Collett B, Ventafridda V, Cohen R, and Gallacher D. Survey of chronic pain in Europe: Prevalence, impact on daily life, and treatment. *European Journal of Pain* 2006 May; 10:287–7. DOI: 10.1016/J.EJPAIN.2005.06.009
2. Treede RD, Rief W, Barke A, Aziz Q, Bennett MI, Benoliel R, Cohen M, Evers S, Finnerup NB, First MB, Giamberardino MA, Kaasa S, Korwisi B, Kosek E, Lavand’Homme P, Nicholas M, Perrot S, Scholz J, Schug S, Smith BH, Svensson P, Vlaeyen JW, and Wang SJ. Chronic pain as a symptom or a disease: The IASP Classification of Chronic Pain for the International Classification of Diseases (ICD-11). *Pain* 2019 Jan; 160:19–27. DOI: 10.1097/J.PAIN.0000000000001384
3. Zolezzi DM, Alonso-Valerdi LM, and Ibarra-Zarate DI. Chronic neuropathic pain is more than a perception: Systems and methods for an integral characterization. *Neuroscience and Biobehavioral Reviews* 2022 May; 136. DOI: 10.1016/J.NEUBIOREV.2022.104599
4. World Health Organization. WHO issues new guidelines on the management of chronic pain in children. 2021
5. Garland EL. Pain Processing in the Human Nervous System: A Selective Review of Nociceptive and Biobehavioral Pathways. *Primary care* 2012 Sep; 39:561. DOI: 10.1016/J.POP.2012.06.013
6. Soysal P, Kalan U, and Arik F. Pain in Older Age. *Encyclopedia of Biomedical Gerontology* 2020 Jan :1–7. DOI: 10.1016/B978-0-12-801238-3.11404-7
7. Mouraux A and Iannetti GD. The search for pain biomarkers in the human brain. *Brain* 2018 Dec; 141:3290–307. DOI: 10.1093/BRAIN/AWY281
8. Van Den Berg B, Vanwinsen L, Pezzali G, and Buitenweg JR. Observation of nociceptive detection thresholds and cortical evoked potentials: Go/no-go versus two-interval forced choice. *Attention, Perception, & Psychophysics* 2022 Apr :1–11. DOI: 10.3758/S13414-022-02484-5
9. Berg B van den, Vanwinsen L, Jansen N, and Buitenweg JR. Real-time estimation of perceptual thresholds based on the electroencephalogram using a deep neural network. *Journal of Neuroscience Methods* 2022 May; 374:109580. DOI: 10.1016/J.JNEUMETH.2022.109580
10. Jiang X, Bian GB, and Tian Z. Removal of Artifacts from EEG Signals: A Review. 2019. DOI: 10.3390/s19050987
11. Islam MK, Rastegarnia A, and Yang Z. Methods for artifact detection and removal from scalp EEG: A review. *Neurophysiologie Clinique* 2016 Nov; 46:287–305. DOI: 10.1016/J.NEUCLI.2016.07.002
12. Lenoir D, Willaert W, Coppieters I, Malfiet A, Ickmans K, Nijs J, Vonck K, Meeus M, and Cagnie B. Electroencephalography During Nociceptive Stimulation in Chronic Pain Patients: A Systematic Review. *Pain Medicine* 2020 Dec; 21:3413–27. DOI: 10.1093/PM/PNAA131

13. Peng W and Tang D. Pain Related Cortical Oscillations: Methodological Advances and Potential Applications. *Frontiers in Computational Neuroscience* 2016 Feb; 10. DOI: 10.3389/FNCOM.2016.00009
14. Lee MC, Mouraux A, and Iannetti GD. Characterizing the Cortical Activity through Which Pain Emerges from Nociception. *Journal of Neuroscience* 2009 Jun; 29:7909–16. DOI: 10.1523/JNEUROSCI.0014-09.2009
15. Nayak CS and Anilkumar AC. EEG Normal Waveforms. *StatPearls* 2021 Jul :1–6
16. Watson BO. Cognitive and Physiologic Impacts of the Infralow Oscillation. *Frontiers in Systems Neuroscience* 2018 Oct; 12:44. DOI: 10.3389/FNSYS.2018.00044
17. Goodman C. Technique for the Analysis of Evoked and Background EEG Activity applied to Young and Elderly Subjects - Doctoral Dissertation of Craig A. Goodman. PhD thesis. 2004
18. Urigüen JA and Garcia-Zapirain B. EEG artifact removal—state-of-the-art and guidelines. *Journal of Neural Engineering* 2015 Apr; 12:031001. DOI: 10.1088/1741-2560/12/3/031001
19. Louis EKS, Frey LC, Britton JW, Frey LC, Hopp JL, Korb P, Koubeissi MZ, Lievens WE, Pestana-Knight EM, and Louis EKS. *Electroencephalography (EEG): An Introductory Text and Atlas of Normal and Abnormal Findings in Adults, Children, and Infants - NCBI Bookshelf*. American Epilepsy Society, 2016
20. Wang ZW, Shi HS, Peng C, and Dabbakuti K. Methods for removal of artifacts from EEG signal: A review. 2020 :12093. DOI: 10.1088/1742-6596/1706/1/012093
21. Kanoga S and Mitsukura Y. Review of Artifact Rejection Methods for Electroencephalographic Systems. *Electroencephalography* 2017 Nov. DOI: 10.5772/68023
22. Ferdousy R, Choudhory AI, Islam MS, Rab MA, and Chowdhory MEH. Electrooculographic and electromyographic artifacts removal from EEG. *ICBEE 2010 - 2010 2nd International Conference on Chemical, Biological and Environmental Engineering, Proceedings* 2010 :163–7. DOI: 10.1109/ICBEE.2010.5651351
23. Zhang S, You B, Lang X, Zhou Y, An F, Dai Y, and Liu Y. Efficient Rejection of Artifacts for Short-Term Few-Channel EEG Based on Fast Adaptive Multidimensional Sub-Bands Blind Source Separation. *IEEE Transactions on Instrumentation and Measurement* 2021; 70. DOI: 10.1109/TIM.2021.3115586
24. McMenamin BW, Shackman AJ, Greischar LL, and Davidson RJ. Electromyogenic artifacts and electroencephalographic inferences revisited. *NeuroImage* 2011 Jan; 54:4–9. DOI: 10.1016/J.NEUROIMAGE.2010.07.057
25. Schlögl A, Keinrath C, Zimmermann D, Scherer R, Leeb R, and Pfurtscheller G. A fully automated correction method of EOG artifacts in EEG recordings. *Clinical Neurophysiology* 2007 Jan; 118:98–104. DOI: 10.1016/J.CLINPH.2006.09.003

26. Croft RJ and Barry RJ. Removal of ocular artifact from the EEG: A review. *Neurophysiologie Clinique* 2000; 30:5–19. DOI: 10.1016/S0987-7053(00)00055-1
27. Chen X, Xu X, Liu A, McKeown MJ, and Wang ZJ. The Use of Multivariate EMD and CCA for Denoising Muscle Artifacts from Few-Channel EEG Recordings. *IEEE Transactions on Instrumentation and Measurement* 2018 Feb; 67:359–70. DOI: 10.1109/TIM.2017.2759398
28. Liu Y, Dai Y, Zhou Y, Lang X, Liu Y, Zheng Q, Zhang Y, Jiang X, Zhang L, and Tang J. An Efficient and Robust Muscle Artifact Removal Method for Few-Channel EEG. *IEEE Access* 2019; 7:176036–50. DOI: 10.1109/ACCESS.2019.2957401
29. Xu X, Chen X, and Yu Z. Removal of muscle artefacts from few-channel EEG recordings based on multivariate empirical mode decomposition and independent vector analysis. *Electronics Letters* 2018 Jul; 54:866–8. DOI: 10.1049/EL.2018.0191
30. Ur Rehman N and Mandic DP. Filter bank property of multivariate empirical mode decomposition. *IEEE Transactions on Signal Processing* 2011 May; 59:2421–6. DOI: 10.1109/TSP.2011.2106779
31. Sun L, Liu Y, and Beadle PJ. Independent component analysis of EEG signals. *Proceedings of the 2005 IEEE International Workshop on VLSI Design and Video Technology, IWVDVT 2005* 2005 :293–6. DOI: 10.1109/IWVDVT.2005.1504590
32. Lin CT, Huang CS, Yang WY, Singh AK, Chuang CH, and Wang YK. Real-Time EEG Signal Enhancement Using Canonical Correlation Analysis and Gaussian Mixture Clustering. *Journal of Healthcare Engineering* 2018; 2018. DOI: 10.1155/2018/5081258
33. Berg B van den and Buitenweg JR. Observation of Nociceptive Processing: Effect of Intra-Epidermal Electric Stimulus Properties on Detection Probability and Evoked Potentials. *Brain Topography* 2021 Mar; 34:139–53. DOI: 10.1007/S10548-020-00816-Y/TABLES/5
34. Gramfort A, Luessi M, Larson E, Engemann DA, Strohmeier D, Brodbeck C, Goj R, Jas M, Brooks T, Parkkonen L, and Hämäläinen M. MEG and EEG data analysis with MNE-Python. *Frontiers in Neuroscience* 2013. DOI: 10.3389/FNINS.2013.00267
35. Thirumalaisamy MR and Ansell PJ. Fast and Adaptive Empirical Mode Decomposition for Multidimensional, Multivariate Signals. *IEEE Signal Processing Letters* 2018 Oct; 25:1550–4. DOI: 10.1109/LSP.2018.2867335
36. Chen X, Liu Q, Tao W, Li L, Lee S, Liu A, Chen Q, Cheng J, McKeown MJ, and Jane Wang Z. ReMAE: User-Friendly Toolbox for Removing Muscle Artifacts from EEG. *IEEE Transactions on Instrumentation and Measurement* 2020 May; 69:2105–19. DOI: 10.1109/TIM.2019.2920186
37. Xu L, Xu M, Ma Z, - A, Zang B, Lin Y, Liu Z, Lawhern VJ, Solon AJ, Waytowich NR, Gordon SM, Hung CP, and Lance BJ. EEGNet: a compact convolutional neural network for EEG-based brain–computer interfaces. *Journal of Neural Engineering* 2018 Jul; 15:056013. DOI: 10.1088/1741-2552/AACE8C